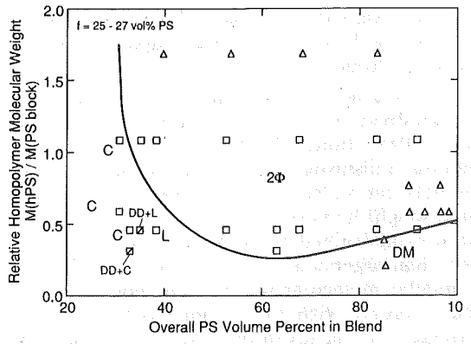

Figure 5. Constant copolymer composition morphology diagram for various homopolystyrenes blended with cylindrical diblock copolymers of f = 25–27 vol % polystyrene: (□) SI13/34 and (△) SB10/23. The solid line denotes the region of macrophase separation in the binary blends.

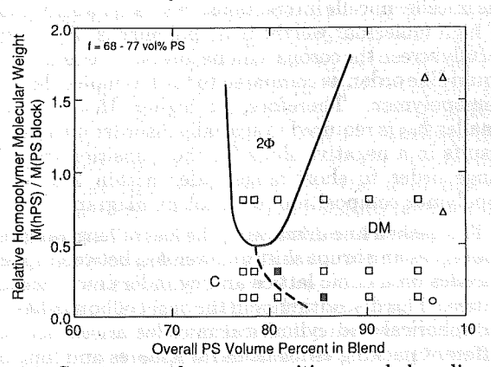

Figure 6. Constant copolymer composition morphology diagram for various homopolystyrenes blended with cylindrical diblock copolymers of f = 68–77 vol % polystyrene: (□) IS12/45, (△) BS10/40, and (○) BS10/23. The solid line denotes the region of macrophase separation, and the dashed line denotes the boundary between ordered and disordered micelles.

Figure 5 exhibits the extensive macrophase-separation behavior which occurs when a homopolymer is blended with the minority component of a diblock copolymer. The macrophase-separation region extends to a relative homopolymer molecular weight of less than 0.5 and spans an overall polystyrene volume percent of 35–100%. The macrophase-separation region of Figure 6, which summarizes the resultant morphologies of blending a homopolymer with the majority component of a diblock copolymer, reaches the $M_{hPS}/M_{PS\ block}$ value of 0.7 but is narrow in the overall PS volume percent in the blend. Together these diagrams for cylindrical diblock copolymers extend the constant copolymer composition morphology diagram for lamellar diblock copolymers (Figure 4) in the third dimension to both lower and higher copolymer compositions. The region of macrophase separation in AB/hA blends enlarges dramatically as the copolymer composition becomes more asymmetric. Similar comparisons between Figures 4–6 can be made with respect to the region of disordered micelles. These preliminary results for the copolymer composition dependence of the constant copolymer composition diagram indicate that a large number of copolymer compositions would have to be studied before a detailed three-dimensional morphology diagram could be constructed.

Conclusions

Isothermal morphology diagrams provide a succinct and insightful means for identifying the morphologies of binary blends and for evaluating the interactions between diblock copolymers and homopolymers. We anticipate that the trends present in these constant molecular weight and the constant copolymer composition morphology diagrams are general features of AB/hA type blends of amorphous polymers. Both types of diagrams illustrate the morphological transitions between ordered morphologies as well as the loss of long-range order. Screening of the corona–corona interactions is promoted by increasing the homopolymer molecular weight and/or the homopolymer concentration.

Acknowledgment. This work was supported by Grant NSF-DMR 89-07433. K.I.W. received support through a NSF Graduate Fellowship and a University of Massachusetts Fellowship.

Supplementary Material Available: Tables of data on constant molecular weight diagrams with 6 hPS and SI, 14 hPS and SI, and 37 hPS and SI and of data on constant copolymer composition diagrams with f = 25–27, 44–51, and 68–77 vol % PS (8 pages). Ordering information is given on any current masthead page.

References and Notes

(1) Kinning, D. J.; Thomas, E. L.; Fetters, L. J. *J. Chem. Phys.* **1989**, *90*, 5806.
(2) Winey, K. I.; Thomas, E. L.; Fetters, L. J. *Macromolecules* **1991**, *24*, 6182.
(3) Winey, K. I.; Thomas, E. L.; Fetters, L. J. *J. Chem. Phys.* **1991**, *95*, 9367.
(4) Winey, K. I.; Thomas, E. L.; Fetters, L. J. *Macromolecules* **1992**, *25*, 422.
(5) Kinning, D. J.; Winey, K. I.; Thomas, E. L. *Macromolecules* **1988**, *21*, 3502.
(6) Winey, K. I.; Thomas, E. L.; Fetters, L. J., to be submitted for publication.
(7) Leibler, L.; Orland, H.; Wheeler, J. C. *J. Chem. Phys.* **1983**, *79*, 3550.
(8) Mayes, A. M.; Olvera de la Cruz, M. *Macromolecules* **1988**, *21*, 2543.
(9) Leibler, L.; Pincus, P. A. *Macromolecules* **1984**, *17*, 2922.
(10) Semenov, A. N. *Macromolecules* **1989**, *22*, 2849.
(11) Whitmore, M. D.; Noolandi, J. *Macromolecules* **1985**, *18*, 2486.
(12) Roe, R.-J.; Zin, W.-C. *Macromolecules* **1984**, *17*, 189.
(13) Helfand, E.; Wasserman, Z. R. In *Developments in Block Copolymers—I*; Goodman, I., Ed.; Applied Science: New York, 1982.
(14) Semenov, A. N. *Sov. Phys. JETP* **1985**, *61*, 733.
(15) Ohta, T.; Kawasaki, K. *Macromolecules* **1986**, *19*, 2621.
(16) Hasegawa, H.; Tanaka, H.; Yamasaki, K.; Hashimoto, T. *Macromolecules* **1987**, *20*, 1651.
(17) Gobran, D. A. Ph.D. Dissertation Thesis, University of Massachusetts, Amherst, MA, 1990.

Registry No. hPS (homopolymer), 9003-53-6; SI (block copolymer), 105729-79-1; SB (block copolymer), 106107-54-4.

Viscoelastic Properties of Immiscible Telechelic Polymer Blends: Effect of Acid–Base Interactions

Pascal Charlier,† Robert Jérôme,* and Philippe Teyssié

Laboratory of Macromolecular Chemistry and Organic Catalysis, University of Liège, Sart-Tilman B6, B-4000 Liège, Belgium

L. A. Utracki

Industrial Materials Research Institute, National Research Council of Canada, Boucherville, Québec, Canada J4B 6Y4

Received October 7, 1991; Revised Manuscript Received January 27, 1992

ABSTRACT: When a telechelic polyisoprene (PIP) end-capped with tertiary amine groups is blended with an immiscible telechelic polystyrene (PS) terminated with either sulfonic or carboxylic acid functions, a proton transfer occurs from the acid to the amine end groups. Viscoelastic properties of these blends support the formation of either ammonium sulfonate or ammonium carboxylate linkages between PS and PIP in a manner analogous to block copolymerization. Due to the low stability of ammonium carboxylates, the related polyblends have been investigated up to 100 °C and they show T_g of each polymeric partner. When PS and PIP chain ends are associated through more thermally stable ammonium sulfonates, the thermal dependences of storage and loss shear moduli show two additional relaxation processes at least in some range of PSand PIP molecular weights. By analogy with SAXS analysis of similar polyblends, these relaxations have been assigned to a classic order–disorder transition similar to that seen in traditional block copolymers and to the irreversible dissociation of the sulfonate salts at higher temperatures, respectively. These additional transitions which involve a change in phase morphology have been confirmed by the "Cole–Cole" log G'' vs log G' plots.

Introduction

Nowadays, the fine tailoring of multiphase polymers is one of the most efficient ways to generate new organic materials of high performance.[1–9] That opportunity has been highlighted for the first time by the poly(styrene-*b*-diene-*b*-styrene) triblock copolymers which behave as thermoreversibly cross-linked rubbers and are commercialized as thermoplastic elastomers.[4] Compared to block copolymerization, melt blending of available polymers using traditional processing equipment is a more convenient way to produce multiphase polymeric materials.[1–3,5–9] Although in these systems each of the partners retains its own properties, the overall physicomechanical behavior is only satisfactory when two demanding structural requirements are met: (i) a controlled microphase separation in relation to a proper interfacial tension and/or appropriate processing conditions; (ii) an interphase adhesion strong enough to assimilate stresses and strains without disruption of the established morphology. Several strategies have been proposed with the view of reaching these targets.[5] Creating a practically irreversible morphology either in the polymerization process itself (e.g., HIPS and ABS resins)[10] or in the blending process is a first possible approach.[5,7,8] A more general strategy consists of using diblock copolymers of tailored structure and molecular weight as interfacial agents.[1,5,11–24] These polymeric additives can lead to excellent properties of the final materials even when used in rather low amounts (ca. 1–2 wt %). Mutual interaction of functional groups randomly attached, one on each immiscible polymer of a binary blend, is another means of controlling interfacial tension and interphase adhesion. Several types of interaction can be promoted, e.g., acid–base, dipole–dipole, ion–ion, and ion–dipole interactions, hydrogen bonding, charge-transfer complexes, and metal–ligand coordination complexes.[25]

The beneficial effect of mutual acid–base interactions on the main characteristics of polyblends has been reported in the scientific literature.[25–30] For instance, ionic cross-interactions between originally immiscible polymers are generated by a proton transfer from acid groups attached to one polymer to amino groups present on the second polymer. For that transfer to be quantitative, pK_a's of the acid and amino groups have to be different by at least 3 units.[25] This is the reason why sulfonic acid/aromatic amine ($\Delta pK_a \simeq 4$) is a commonly used acid/base pair. The effect promoted by the mutually interacting groups depends on their concentration. Below a critical value (5 mol % with respect to the monomeric units of the modified polymer), polystyrene/poly(ethyl acrylate) and polystyrene/polyisoprene blends are opaque and show two T_g's, although their mechanical properties are improved. Above the critical ionic content, blends are transparent and exhibit a unique T_g which is, however, observed as a broad relaxation peak by mechanical measurements, suggesting that miscibility does not exist at a scale smaller than 10 nm.[25] Spectroscopic and mechanical studies on blends of sulfonic acid containing polystyrene and polyurethane also show that a proton transfer takes place from the sulfonic acid groups to the urethane moieties.[31–33] Interestingly enough, when used at a rate of at least 13 mol %, carboxylic acid and pyridine units are able to promote the miscibility of poly(methyl methacrylate) (PMMA) and poly(butyl acrylate).[34] A positive effect of hydrogen bonding has also been reported for blends of poly(2-vinylpyridine) and poly(ethylene-*co*-methacrylic acid).[35] Finally, carboxylic acid–urethane interactions are likely to occur since mechanical properties of polystyrene/polyurethane blends are improved when polystyrene is modified by carboxylic acid groups.[36,37]

Proton transfer from acid end groups of one telechelic polymer to dimethylamine end groups of an immiscible

* To whom correspondence should be addressed.
† Present address: Machelen Chemical Technology Center, Exxon Chemical International Inc., 2, Nieuwe Nijverheidslaan, B-1831 Machelen, Belgium.

0024-9297/92/2225-2651$03.00/0

telechelic partner has been investigated as a model system for the more complex situation in which intermolecular ionic bonding or hydrogen bonding is promoted by interactive moieties distributed at random along the polymeric backbones.[38-42] Since the spontaneous trend of the blended polymers to demix is counterbalanced now by cross-interactions between the chain ends of each polymeric component, these mixtures are expected to mimic closely the phase morphology and general properties of the corresponding multiblock copolymers. That analogy has been substantiated by several techniques. IR spectroscopy[38,41] supports the occurrence of proton transfer from carboxylic acid to dimethylamine end groups with the formation of "interchain" ammonium carboxylate ion pairs (eq 1). Optical microscopy shows that the phase

$$\sim\!PA\!\sim\!COOH + R_2N\!\sim\!PB\!\sim \rightarrow \left[\sim\!PA\!\sim\!COO^- \; R_2\overset{+}{N}H\!\sim\!PB\!\sim\right] \quad (1)$$

separation of PA and PB is controlled by the ion pairs bridging the chain extremities to a level that depends (i) on the nature of PA and PB and their intrinsic immiscibility, (ii) on the ion pair content, in relation to molecular weight of PA and PB, and (iii) on the strength of the ion pairs, ammonium sulfonates being more effective in fighting the immiscibility of PA and PB than ammonium carboxylates.[41] T_g measurements are in qualitative agreement with the general pattern reported for multiphase block polymers.[38,41] The solution viscosity of PA and PB telechelic polymer blends in a common, apolar solvent is significantly modified by the ionic bonding between the polymers and the possible dipolar interactions of the bridging ion pairs.[41] Finally a temperature-dependent small-angle X-ray scattering study has shown that the morphology of the polyblends closely resembles that seen in covalently bonded block copolymers.[39] When ammonium sulfonate ion pairs are concerned and depending on the molecular weight of PA and PB, a classic order–disorder transition is observed and even possibly followed by the effect of a critical solution temperature. This paper deals with the viscoelastic properties of blends of α,ω-bis(dimethylamino)polyisoprene [$PIP(NR_2)_2$] and α,ω-dicarboxy- or -disulfopolystyrene [$PS(COOH)_2$ or $PS(SO_3H)_2$]. The effect of the bridging ion pairs and their strength and content will be considered, and the dynamic mechanical behavior will be related as much as possible to the phase morphology previously investigated by SAXS.

Experimental Section

Sample Preparation. Telechelic polymers were prepared by anionic polymerization. Pure and carefully dried monomers and solvents were used. Isoprene and styrene were dried over CaH_2 at room temperature and distilled under reduced pressure just before use. Isoprene and styrene were mixed with *n*-butyllithium and lithium fluorenyl, respectively, and again distilled before polymerization.

Polymerization was performed in previously flamed and nitrogen-purged flasks equipped with rubber septums. Hypodermic syringes and stainless-steel capillaries were used to handle liquid products under a nitrogen atmosphere. α,ω-Bis(dimethylamino)polyisoprene was anionically prepared in THF, at −78 °C, using sodium naphthalene as a difunctional initiator. α,ω-Disulfopolystyrene was prepared under the same experimental conditions except for the counterion of the active species which was Li instead of Na. The initiators resulted from the reaction of naphthalene with a slight excess of the appropriate alkaline metal in THF at room temperature.

The living macrodianions were deactivated by anhydrous carbon dioxide,[43] 1,3-propane sultone,[44] and 1-chloro-3-(dimethylamino)propane[45] with the formation of α,ω-dicarboxypolystyrene [$PS(COOH)_2$], α,ω-disulfopolystyrene [$PS(SO_3OH)_2$], and α,ω-bis(dimethylamino)polyisoprene [$PIP(NMe_2)_2$], respectively.

Table I
Molecular Characteristics of Telechelic Polymers

sample	$\bar{M}_n \times 10^{-3}$	$\bar{M}_w/\bar{M}_n$	$\bar{M}_t$,[a] $\times 10^{-3}$	f[b]
$PIP(NMe_2)_2$ 18K	18.0	1.2	19.5	1.85
$PIP(NMe_2)_2$ 38K	38.4	1.3	41.5	1.86
$PS(COOH)_2$ 13K	13.2	1.4	13.5	1.96
$PS(SO_3H)_2$ 9K	9.1	1.3	10.0	1.82
$PS(SO_3H)_2$ 15K	14.6	1.2	15.8	1.85

[a] $\bar{M}_t$ = molecular weight determined by titration of the end groups.[37] [b] f = functionality = $2\bar{M}_n/\bar{M}_t$.

Table II
Compositions and Code Names of Blends of Telechelic Polymers

blends[a]	code name
$PIP(NMe_2)_2$ 38K–$PS(COOH)_2$ 13K	M38–13C
$PIP(NMe_2)_2$ 38K–$PS(SO_3H)_2$ 9K	M38–9S
$PIP(NMe_2)_2$ 38K–$PS(SO_3H)_2$ 15K	M38–15S
$PIP(NMe_2)_2$ 18K–$PS(COOH)_2$ 13K	M18–13C
$PIP(NMe_2)_2$ 18K–$PS(SO_3H)_2$ 9K	M18–9S
$PIP(NMe_2)_2$ 18K–$PS(SO_3H)_2$ 15K	M18–15S

[a] PIP/PS = 1/1 (mol/mol).

The microstructure of the polyisoprene was found to be a mixture of 1,2/3,4 in a ratio of 35/65. Molecular weights of the telechelics were controlled by adjusting the monomer to initiator molar ratio. The molecular weight and polydispersity of the telechelic polymers were measured by size-exclusion chromatography (SEC), as reported elsewhere.[45] The functionality was calculated from the $\bar{M}_n$ value (SEC) and from the potentiometric titration of the end groups. Dimethylamino groups and acid groups (COOH and SO_3H) were titrated with perchloric acid and tetramethylammonium hydroxide, respectively, in a 9/1 toluene/methanol mixture. Polyisoprene was carefully stabilized by an antioxidant (1 wt % of Irganox 1010).

The main molecular characteristics of telechelic polymers are reported in Table I.

Polymer blends were prepared by means of solvent-casting techniques. Separate solutions of each polymer in a 9/1 toluene/methanol mixture were prepared. After having mixed the proper volumes of each solution (so that the acid/amine molar ratio was 1), the solutions were allowed to stir for 24 h before casting. Films were prepared by a slow evaporation of the solvent followed by vacuum drying to constant weight at 70 °C (ca. 1 month). Samples for dynamic mechanical measurements were prepared by compression molding at 2 MPa and 140 °C for 20 min. Table II summarizes the compositions of the blends investigated in this study together with their code names.

Differential Scanning Calorimetry (DSC). DSC thermograms were recorded, from −40 up to +200 °C. Samples were previously annealed at 200 °C for 15 min. A Perkin-Elmer DSC-4 was used at a heating rate of 20 °C/min under a constant flow of dry nitrogen.

Dynamic Mechanical Measurements. A Rheometrics mechanical spectrometer (RMS 605S) was used with a parallel-plate geometry. The 25-mm-diameter specimen in a 1.4-mm-wide gap was tested under a constant flow of dry nitrogen. Measurement were carried out at a constant frequency (ν = 1 Hz) and a constant heating/cooling rate of 2 °C/min. Isothermal frequency scans at frequencies from 0.016 to 16 Hz were conducted for M38–13C and M18–15S blends.

Results and Discussion

Effect of Strength of the Ion Pairs and of Their Mutual Interactions. Figures 1–3 illustrate the thermal dependence of the storage (G') and loss (G'') shear moduli, measured at a frequency of 1 rad s^{-1} for blends containing $PIP(NR_2)_2$ 38K (where 38K refers to molecular weight) associated to PS $(SO_3H)_2$ 15K, $PS(SO_3H)_2$ 9K, and PS $(COOH)_2$ 13K, respectively.

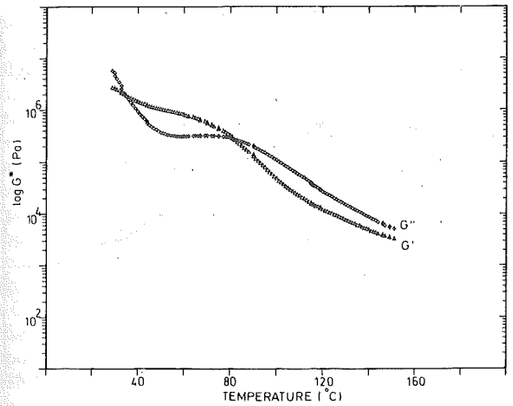

Figure 1. Storage (G') and loss (G'') shear moduli vs temperature (1 Hz) for the M38–15S blend (Table II).

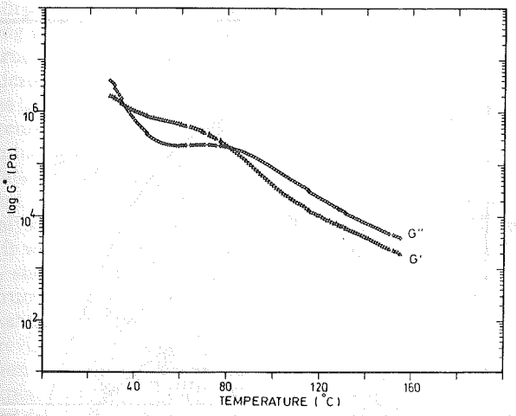

Figure 2. Storage (G') and loss (G'') shear moduli vs temperature (1 Hz) for the M38–9S blend (Table II).

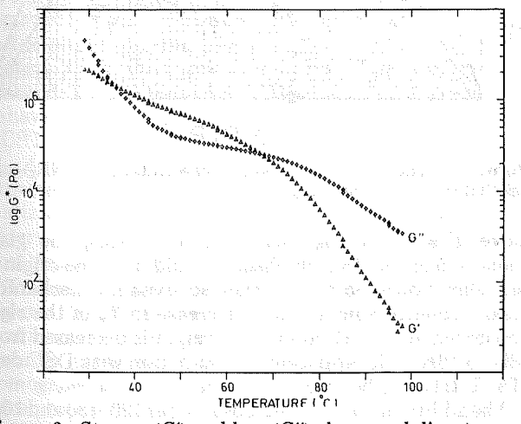

Figure 3. Storage (G') and loss (G'') shear moduli vs temperature (1 Hz) for the M38–13C blend (Table II).

All the G'' curves show a maximum in the temperature range of 70–80 °C. Such a relaxation has been assigned to the glass transition of polystyrene (or polystyrene-rich) phases. Above that transition temperature, the material clearly starts to flow. That interpretation assumes that the investigated blends are phase separated. This has been confirmed elsewhere[41] and shown in this study by differential scanning calorimetry (DSC). Indeed, two T_g's are reported (Table III) which compared to T_g of the parent PIP and PS are characteristic of phases of that nature. The difference in the T_g's for each type of phase is also mentioned in Table III. ΔT_g is smaller by ca. 10 °C when

Table III
T_g's of Telechelic Polymers and Binary Blends

sample	T_{g1}, °C	T_{g2}, °C	ΔT_g[b]
PIP 18K[a]	3		
PIP 38K[a]	17		
PS 9K[a]		95	
PS 13K[a]		97	
PS 15K		98	
M38–13C	17	112	95
M38–15S	20	108	88
M38–9S	19	107	88
M18–13C	14	113	99
M18–15S	18	106	88
M18–9S	18	105	87

[a] Polymer free from functional end groups. [b] $\Delta T_g = T_{g2} - T_{g1}$.

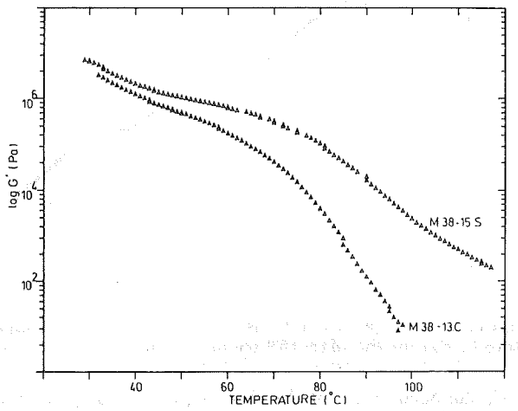

Figure 4. Comparison of the log G' vs temperature curve (1 Hz) for M38–15S and M38–13C blends (Table II).

the chain ends are held together through ammonium sulfonate ion pairs rather than carboxylate ones. This indicates that an increase in the strength of the bridging ion pairs is in favor of an improved miscibility, all the other conditions being unchanged.

Figure 4 compares the G' curves for two blends M38–15S and M38–13C which essentially differ on the nature of the acid end groups.

The intermediate plateau below 70–80 °C extends over a larger temperature range, and G' of that plateau is higher when PS is end-capped by a sulfonic acid. These observations mean that ammonium sulfonates are stronger dipoles than their carboxylate counterparts and that their mutual interactions stabilize a stronger chain network. Indeed the telechelic polymer blends under investigation can be depicted not only as an ionically bonded block copolymer but also as a two-component (PS and PIP) ionomer of the sulfonic type. In this regard, it is well-known that the mutual association of sulfonate ion pairs improves the high-temperature properties of the ionomer much more effectively than carboxylate dipoles do.[46]

At 70 °C, the M38–13C blend starts to flow rapidly which reflects the fast disruption of the mutual association of the ammonium carboxylate ion pairs and most likely the thermal rupture of the ion pairs themselves with release of the carboxylic acid and dimethylamine end groups. It is worth pointing out that a $PS(COOH)_2$ 13K sample has been previously neutralized with triethylamine and then heated at 130 °C under vacuum. The back proton transfer has been observed as supported by the quantitative elimination of triethylamine[47,48] (eq 2). In contrast to M38–

$$PS(COO^- \; {}^+HNR_3)_2 \xrightarrow[\text{in vacuo}]{130\ ^\circ C} PS(COOH)_2 + 2NR_3 \quad (2)$$

Table IV
Molar and Weight Compositions of Binary Blends of Telechelic Polymers

	PIP		PS		$SO_3^-N^+$:
code name	mol %[a]	wt %	mol %[a]	wt %	mol %[a]
M38–15S	79.3	71.7	20.4	28.3	0.28
M38–9S	86.3	80.9	13.4	19.1	0.31
M18–15S	64.4	54.5	35.1	45.5	0.49
M18–9S	74.9	66.7	24.5	33.3	0.57

[a] On the basis of the monomer content.

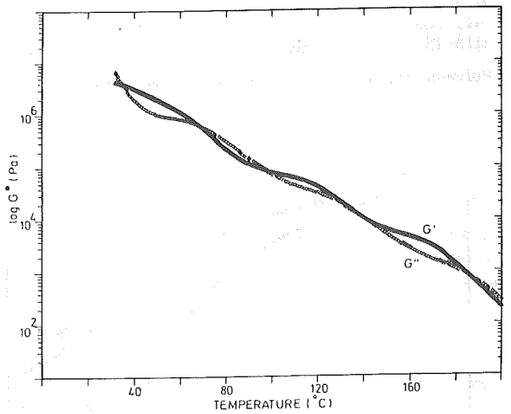

Figure 5. Storage (G') and loss (G'') shear moduli vs temperature (1 Hz) for the M18–15S blend (Table II).

13C, the occurrence of the flow regime is delayed in the M38–15S blend and the decrease in G' at increasing temperature is much slower. For instance, the complex shear modulus of M38–15S is easily measured at 150 °C (Figure 1) whereas it is already too small to be measured accurately at 100 °C for the M38–13C mixture (Figure 3). This is the consequence of the highest thermal stability of the ammonium sulfonate ion pairs compared to the carboxylate ones.[47,48]

Effect of the Ion Pair Content. In the previous blends, the molecular weight of $PS(SO_3H)_2$ associated to $PIP(NH_2)_2$ 38K was changed from 15K to 9K and no substantial modification in the viscoelastic behavior was noted (see Figures 1 and 2). It must, however, be stressed that the ion pair content remained essentially unaffected as calculated in Table IV. This is the reason why a second series of blends was prepared in which the molecular weight of $PIP(NH_2)_2$ was made to decrease by a factor of 2. Accordingly, the ion pair content was increased by ca. 80% with respect to samples of the first series (Table IV).

Figures 5 and 6 show the G' and G'' curves for the M18–15S and M18–9S mixtures which are basically different from those reported for the related blends containing $PIP(NR_2)_2$ of a twice as high molecular weight (Figures 1 and 2). Actually, two additional transitions are observed on the high-temperature side. In order to assign the relaxation processes observed in the investigated temperature range, it is worth referring to T_g data of Table II. In spite of a substantial increase in the ion pair content, the telechelic polymer blends are still phase separated and the T_g of each phase as measured by DSC is not significantly modified. According to the G'' curves of Figures 5 and 6, the first maximum on the low-temperature side is observed at 65 °C and the next one at 120–130 °C. One of these maxima should be attributed to the T_g of polystyrene-rich phases. The decrease in the PIP molecular weight together with the increase in the content of the ion pairs which have to accumulate in the interfacial region is expected to enhance the polymer miscibility and

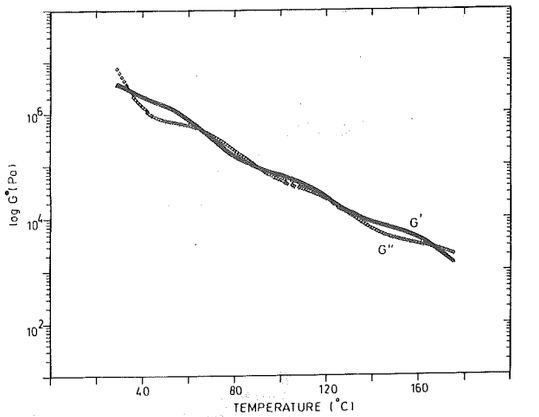

Figure 6. Storage (G') and loss (G'') shear moduli vs temperature (1 Hz) for the M18–9S blend (Table II).

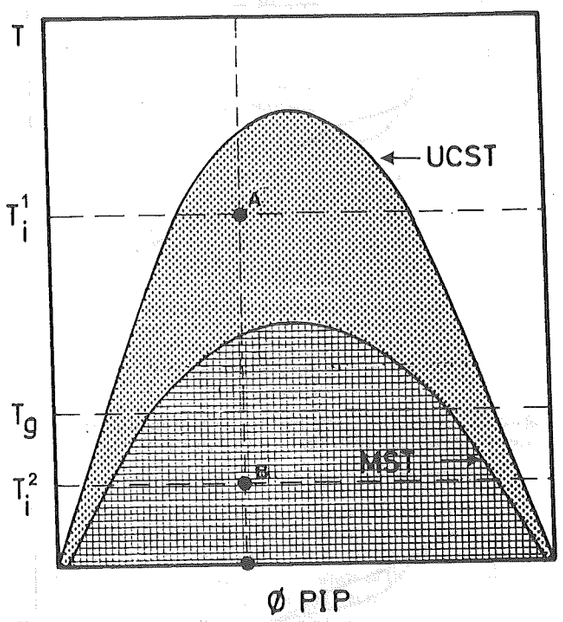

Figure 7. Schematic phase diagram of blends of $PIP(NR_2)_2$ and $PS(COOH)_2$ or $PS(SO_3H)_2$.[35]

move T_g's closer together. On that basis, the glass transition of the PS-rich phases should be at the origin of the relaxation at 65 °C. If this is so, dynamic mechanical measurements conclude to a decrease in T_g of the rigid phases when the PIP molecular weight is decreased from 38K to 18K. The apparent contradiction with DSC data (Table III) will be discussed later.

The additional relaxations observed at 120–130 and 160–180 °C, respectively, have something to do with the sulfonate ion pairs and their association, since polystyrene ionomers of the sulfonic type exhibit an ionic relaxation in that range of temperature.[49] It is, however, of great significance to refer now to a previous study on the thermal dependence of the SAXS profile of blends comprising $PIP(NR_2)_2$ 18K and α,ω-disulfopoly(α-methylstyrene) of various molecular weights.[39] From that study, the general phase diagram schematized in Figure 7 has been proposed where UCST is the upper critical solution temperature of the constituent telechelic polymers, MST is the microphase-separation temperature of the ionic copolymers, T_g is the glass transition of the hard phases, and T_i is the temperature at which the bridging ion pairs forming the

block copolymers are disrupted. T_i depends on the strength of the ion pairs, the intrinsic immiscibility of the polymer pair, and the molecular weight of each of them. When T_i is above both T_g and the MST curve (representative system A), an order–disorder transition occurs when the microphase-separated system goes across the MST curve and a uniform melt is observed. At higher temperatures, i.e., greater than T_i, the effective homogeneous copolymer melt is broken up into the constituent homopolymers and phase separation of the homopolymers occurs. The two additional relaxation mechanisms of Figures 5 and 6 could now be accounted for. The maximum in G'' at 120–130 °C should correspond to the classical order–disorder transition seen in covalently bonded block copolymers. In the investigated blends (M18–15S and M18–9S), that transition is actually triggered by the relaxation of the ion pair association.[50–53] In other words, the mutual interactions of the ammonium sulfonate ion pairs are unable to stabilize a microphase-separated morphology at temperatures higher than 120–130 °C. As long as the ion pairs are stable, chains retain a "blocky" structure and the system remains homogeneous at the microscopic level. At higher temperatures (160–180 °C) the thermal breakup of the ammonium sulfonate ion pairs occurs together with a release of sulfonic acid and tertiary amine end groups, resulting in a macrophase separation. This is supported by the elsewhere-reported observation that ammonium sulfonates attached at the end of a polystyrene chain are unstable above 180 °C.[47,48] Since it is well-known that aliphatic sulfonic acids are unstable at such high temperatures, the ionic block copolymer structure is irreversibly lost. It is now worth mentioning that the samples analyzed by DSC in this study have been previously annealed at 200 °C in order to make them free from any residual solvent. That pretreatment might explain the discrepancy in T_g values determined by DSC and dynamic mechanical measurements. When the high-temperature pretreatment is not applied, data provided by the two methods are consistent.[41] The G' and G'' curves reported in Figures 1–3 can also be rationalized by referring to the phase diagram of Figure 7 where B is the representative system. Since T_i is below T_g, as soon as T_g is reached, the components of the ionic block copolymer behave as individual homopolymer molecules below the UCST and coarse phase separation ensues. Thus, above T_g of the rigid PS phases, no additional relaxation is expected to occur, as is actually observed. Figure 8 schematizes the three main phase situations which can be observed when ion pairs associate the chain ends of immiscible telechelic polymers.

Transitions observed at 120–130 and 160–180 °C in Figures 5 and 6 have been assigned to relaxation processes that involve a change in the phase morphology: an order–disorder transition and a macrophase separation of a homogeneous system. Very interestingly, Han et al.[54–56] have proposed a method which has proven to be fruitful in giving prominence to the order–disorder transition in poly(styrene-*b*-isoprene-*b*-styrene) copolymers.[57] The method consists of first recording the isothermal dependence of G' and G'' on frequency and then plotting log G'' versus log G'. These graphs are actually Cole–Cole plots on a log–log scale. As long as the morphology remains unchanged in the investigated temperature range, isothermal log G'' vs log G' curves superimpose with formation of a single "master curve".[54] In contrast, when the phase morphology is modified, the superposition fails at least until it becomes again temperature independent. On the basis of that criterion, the Cole–Cole plot of Figure 9 shows that the morphology of the M38–13C mixture is preserved from 40 up to ca. 100 °C, i.e., up to the origin of the viscous

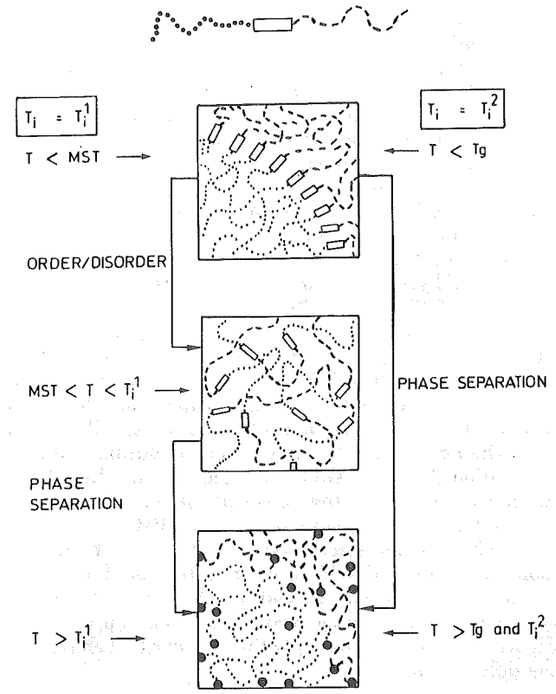

Figure 8. Representation of the main phase situations observed in blends of immiscible telechelic polymers, where –□– schematizes an ammonium carboxylate ($-COO^-R_2^+NH-$) or sulfonate ($-SO_3^-R_2^+NH-$) ion pair.

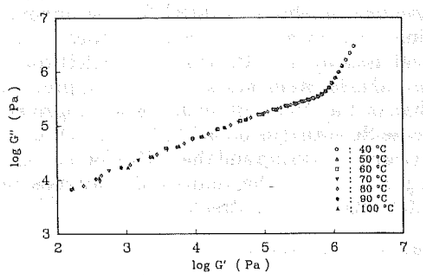

Figure 9. log G' vs log G'' curves for the M38–13C blend (Table II).

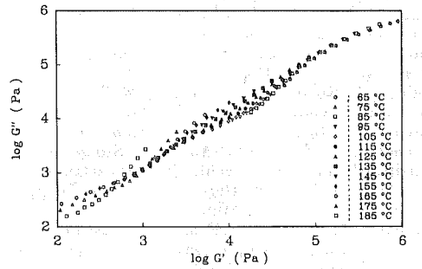

Figure 10. Cole–Cole plot for the M18–15S blend (Table II).

flow regime. Thus, as long as T_g of the PS phases is not exceeded, the two-phase structure is stabilized by that rigid PS component in agreement with Figure 7 (representative system B). When the M18–15S blend is concerned, the situation radically changes, as illustrated by Figure 10. The superposition of the log G'' vs log G' curves does not fit in two temperature ranges. The first one extends approximately from 115 to 155 °C, which corresponds satisfactorily to the second relaxation seen in Figure 5. The Cole–Cole plot gives accordingly credit to

the assignment of an order–disorder transition to that relaxation. The same conclusion can be drawn for the second temperature range in which superposition of the Cole–Cole plot does not work (i.e., above ca. 165 °C), since it fits the third relaxation observed in the viscoelastic curves of Figure 5 and substantiates the attribution of a macroscopic phase demixing.

In conclusion, there is a very good agreement between the viscoelastic properties of blends of α,ω-bis(dimethylamino)polyisoprene and α,ω-dicarboxy- or -disulfopolystyrene and the phase morphology which has been determined by SAXS for analogous blends.[39] The relative positions of T_g of the PS phases, the order–disorder transition temperature of the bridging ion pairs (T_i), and the MST curve play a key role. That situation can interestingly be controlled by (i) the intrinsic strength of the ion pairs (ammonium carboxylates against sulfonates) which affects the partial miscibilitity of PS and PIP (thus T_g of the PS phase), the strength of the mutual ion pair association (thus the MST value), and T_i and by (ii) the molecular weight of the telechelic polymers, i.e., the thermodynamic repulsion of PS and PIP which acts adversely onto the electrostatic interactions of the ammonium cation and sulfonate (or carboxylate) anion, as well as on their mutual association. As a result, it is quite possible to go through the whole phase diagram shown on Figure 7 and to change deeply the viscoelastic behavior of the polyblends.

Acknowledgment. P.C., R.J., and Ph.T. are very much indebted to the "Service de la Programmation de la Politique Scientifique" and the "Fonds National de la Recherche Scientifique" (FNRS) for financial support. P.C. is very much indebted to IMRI for the opportunity of spending a 3-month stay in their facilities. The skillful technical assistance of P. Sammut (IMRI) for dynamic mechanical measurements is very much appreciated. P.C. also thanks the "Institut pour l'Encouragement de la Recherche Scientifique dans l'Industrie et l'Agriculture" (IRSIA) for a fellowship and the FNRS for having awarded him a grant to visit the Industrial Materials Research Institute (IMRI) of Montreal.

References and Notes

(1) Teyssié, Ph.; Fayt, R.; Jérôme, R. *Makromol. Chem., Macromol. Symp.* **1988**, *16*, 41.
(2) Utracki, L. A. *Int. Polym. Process.* **1987**, *2*, 3.
(3) Schreiber, P.; Latham, J. *Polym. News* **1987**, *13*, 19.
(4) Legge, N. R., Holden, G., Schroeder, H. E., Eds. *Thermoplastic Elastomers*; Hanser: Munich, 1987.
(5) Paul, D. R., Newman, S., Eds. *Polymer Blends*; Academic Press: New York, 1978; Vols. 1 and 2.
(6) Olabisi, O.; Robeson, L. M.; Shaw, M. T. *Polymer–Polymer Miscibility*; Academic Press: New York, 1979.
(7) Walsh, D. J.; Higgins, J. S. *Polymer Blends and Mixtures*; Maconnachie, A., Ed.; NATO Advanced Study Institute Series; Martinus Nijhoff: Dordrecht, The Netherlands, 1985.
(8) Utracki, L. A. *Polymer Alloys and Blends, Thermodynamics and Rheology*; Hanser: Munich, 1989.
(9) Utracki, L. A., Weiss, R. A., Eds. *Multiphase Polymers: Blends and Ionomers*; ACS Symposium Series 395; American Chemical Society: Washington, DC, 1989.
(10) Bucknall, C. B. *Toughened Plastics*; Applied Science: London, 1977.
(11) Fayt, R.; Jérôme, R.; Teyssié, Ph. *J. Polym. Sci., Polym. Lett.* **1981**, *19*, 79; **1986**, *24*, 25.
(12) Fayt, R.; Jérôme, R.; Teyssié, Ph. *J. Polym. Sci., Polym. Phys. Ed.* **1981**, *19*, 1269; **1982**, *20*, 2209; **1989**, *27*, 775.
(13) Fayt, R.; Jérôme, R.; Teyssié, Ph. *Makromol. Chem.* **1986**, *187*, 837.
(14) Fayt, R.; Jérôme, R.; Teyssié, Ph. *Polym. Eng. Sci.* **1987**, *27*, 328.
(15) Fayt, R.; Jérôme, R.; Teyssié, Ph. *J. Appl. Polym. Sci.* **1986**, *32*, 5647.
(16) Fayt, R.; Teyssié, Ph. *Macromolecules* **1986**, *19*, 2077.
(17) Ouhadi, T.; Fayt, R.; Jérôme, R.; Teyssié, Ph. *J. Polym. Sci., Polym. Phys. Ed.* **1986**, *24*, 973.
(18) Ouhadi, T.; Fayt, R.; Jérôme, R.; Teyssié, Ph. *Polym. Commun.* **1986**, *27*, 212.
(19) Ouhadi, T.; Fayt, R.; Jérôme, R.; Teyssié, Ph. *J. Appl. Polym. Sci.* **1986**, *32*, 5647.
(20) Heuschen, J.; Vion, J. M.; Jérôme, R.; Teyssié, Ph. *Polymer* **1990**, *31*, 1473.
(21) Barlow, J. W.; Paul, D. R. *Polym. Eng. Sci.* **1984**, *24*, 525.
(22) Anastasiadis, S. H.; Gancarz, I.; Koberstein, J. T. *Macromolecules* **1989**, *22*, 1449.
(23) Shull, K. R.; Kramer, E. J.; Hadziioannou, G.; Tang, W. *Macromolecules* **1990**, *23*, 4780.
(24) Cho, K.; Brown, H. R.; Miller, D. C. *J. Polym. Sci., Part B: Polym. Phys.* **1990**, *28*, 1699.
(25) Smith, P.; Hara, M.; Eisenberg, A. *A Review of Miscibility Enhancement via Ion–Ion and Ion–Dipole Interactions. Current Topics in Polymer Science*; Hanser: New York, 1987; Vol. 2, Part 6.
(26) Eisenberg, A.; Smith, P.; Zhou, Z. L. *Polym. Eng. Sci.* **1982**, *22*, 1117.
(27) Smith, P.; Eisenberg, A. *J. Polym. Sci., Polym. Lett. Ed.* **1983**, *21*, 223.
(28) Zhou, Z. L.; Eisenberg, A. *J. Polym. Sci., Polym. Phys. Ed.* **1983**, *21*, 595.
(29) Bazuin, C. G.; Eisenberg, A. *J. Polym. Sci., Polym. Phys. Ed.* **1986**, *24*, 1021.
(30) Murali, R.; Eisenberg, A. *J. Polym. Sci., Polym. Phys. Ed.* **1988**, *26*, 1385.
(31) Rutkowska, M.; Eisenberg, A. *Macromolecules* **1984**, *17*, 821.
(32) Tannenbaum, R.; Rutkowska, M.; Eisenberg, A. *J. Polym. Sci., Polym. Phys. Ed.* **1987**, *25*, 663.
(33) Natansohn, A.; Murali, R.; Eisenberg, A. *Makromol. Chem., Makromol. Symp.* **1988**, *16*, 175.
(34) Jo, W. H.; Lee, S. C.; Lee, M. S. *Polym. Bull.* **1989**, *21*, 183.
(35) Lee, J. Y.; Painter, P. C.; Coleman, M. M. *Macromolecules* **1988**, *21*, 954.
(36) Hsieh, K. H.; Wu, M. L. *J. Appl. Polym. Sci.* **1989**, *37*, 347.
(37) Hsieh, K. H.; Chou, L. M.; Chiang, Y. C. *Polym. J.* **1989**, *21*, 1.
(38) Horrion, J.; Jérôme, R.; Teyssié, Ph. *J. Polym. Sci., Polym. Lett. Ed.* **1986**, *24*, 69.
(39) Russel, T. T.; Jérôme, R.; Charlier, P.; Foucart, M. *Macromolecules* **1988**, *21*, 1709.
(40) Horrion, J.; Jérôme, R.; Teyssié, Ph.; Vanderschueren, J.; Corapci, M. *Polym. Bull.* **1989**, *21*, 627.
(41) Horrion, J.; Jérôme, R.; Teyssié, Ph. *J. Polym. Sci., Polym. Chem. Ed.* **1990**, *28*, 153.
(42) Charlier, P.; Jérôme, R.; Teyssié, Ph.; Utracki, L. A. *Polym. Networks Blends* **1991**, *1*, 27.
(43) Broze, G.; Jérôme, R.; Teyssié, Ph. *Macromolecules* **1982**, *15*, 920.
(44) Foucart, M. Ph.D. Thesis, University of Liège, Belgium, 1988.
(45) Charlier, P.; Jérôme, R.; Teyssié, Ph. *Macromolecules* **1990**, *23*, 1831.
(46) Lundberg, R. D.; Makowski, H. S. *Adv. Chem. Ser.* **1980**, *187*, 21.
(47) Charlier, P. Ph.D. Thesis, University of Liège, Belgium, 1990.
(48) Charlier, P.; Jérôme, R.; Teyssié, Ph.; Prud'homme, R. E., to be published.
(49) Bazuin, C. G.; Eisenberg, A. *Ind. Eng. Chem. Prod. Res. Dev.* **1981**, *20*, 271.
(50) Chung, C. I.; Lin, M. I. *J. Polym. Sci., Polym. Phys. Ed.* **1978**, *16*, 545.
(51) Widmaier, J. M.; Meyer, G. C. *J. Polym. Sci., Polym. Phys. Ed.* **1980**, *18*, 2217.
(52) Roe, R. J.; Fishkis, M.; Chang, J. C. *Macromolecules* **1981**, *14*, 1091.
(53) Kraus, G.; Hashimoto, T. *J. Appl. Polym. Sci.* **1982**, *27*, 1745.
(54) Han, C. D.; Kim, J. *J. Phys. Sci., Polym. Phys. Ed.* **1987**, *25*, 1741.
(55) Kim, J.; Han, C. D. *J. Polym. Sci., Polym. Phys. Ed.* **1988**, *26*, 677.
(56) Han, C. D.; Kim, J.; Kim, J. K. *Macromolecules* **1989**, *22*, 383.
(57) Han, C. D.; Back, D. M.; Kim, J. K. *Macromolecules* **1990**, *23*, 561.

Self-Consistent Field Theories for Polymer Brushes. Lattice Calculations and an Asymptotic Analytical Description

C. M. Wijmans* and J. M. H. M. Scheutjens

Department of Physical and Colloid Chemistry, Wageningen Agricultural University, Dreijenplein 6, 6703 HB Wageningen, The Netherlands

E. B. Zhulina

Institute of Macromolecular Compounds, Russian Academy of Science, St. Petersburg 199004, Russia

Received October 18, 1991; Revised Manuscript Received January 30, 1992

ABSTRACT: In this paper we compare two models for calculating the configuration of grafted polymer chains at a solid-liquid interface. The first model is the self-consistent field (SCF) polymer adsorption theory of Scheutjens and Fleer as extended for end-attached chains. In this approach the equilibrium distribution of the polymer is found by averaging the statistical weights of all possible chain conformations that can be generated on a lattice. The second model is an analytical SCF theory developed independently by Zhulina, Borisov, and Priamitsyn and by Milner, Witten, and Cates which predicts the grafted layer structure in the case of strong chain stretching. A comparison is made between the results of both theories, and the deviations are explained from the assumptions made in the less exact analytical theory.

1. Introduction

Polymer chains that are grafted at one end onto an impenetrable surface form a good model for the analysis of numerous systems, such as sterically stabilized colloidal dispersions, block copolymer surfactants at solid–liquid and liquid–liquid interfaces, solutions and melts of block copolymers under the conditions in which microphases are formed, etc. Theoretical analysis of grafted chain layers was initiated by the pioneering work of Alexander.[1] Using scaling arguments,[1–3] the main features of grafted layers were established, particularly the considerable stretching of overlapping chains perpendicular to the grafting surface. This stretching is greatest for the case of a planar grafted layer, so that the thickness of the layer H is proportional to N for solvents of various strengths. This scaling relationship between the layer thickness and the degree of polymerization suggested the picture of a mainly homogeneous layer of constant concentration and at the periphery of the layer a rapid decrease of concentration.

Further progress in the analytical theory of grafted layers was attained using the self-consistent field (SCF) approach proposed by Semenov.[4] This approach is based on assuming large stretching of the grafted chains with respect to their Gaussian dimension to allow the replacement of the set of conformations of a stretched grafted chain by their "average trajectory" (the so-called Newton or strong-stretching approximation) which significantly simplifies the description of the system. This idea was first applied by Semenov to dense grafted layers (i.e., layers without solvent) and led to a very elegant theory of super structure formation in block copolymer melts under strong segregation conditions.

This SCF approach was generalized and applied to grafted polymer layers immersed in low molecular weight solvents[5,6] and solutions or melts of mobile polymers.[7] Many effects were considered, such as the collapse of the layer due to a decrease of the solvent strength,[8] the polydispersity of grafted and mobile chains,[9] deformational[10] and dynamical[11] behavior of grafted layers, etc.

These investigations led to a different picture of the grafted layer structure. The polymer concentration decreases monotonically on going from the surface to the outside of the layer. Furthermore, the free chain ends are distributed throughout the whole layer. The system parameters such as solvent quality, polydispersity, etc., appear to strongly influence the shapes of the volume fraction profile and the free chain end distribution.

The development of an analytical theory was accompanied by investigations of grafted layers by Monte Carlo simulations[12–15] and numerical calculations using a SCF lattice model.[12,16] In the latter method, the equilibrium concentration profile of the grafted layer is found by accounting for all the possible conformations of the polymer chains that can be generated on a planar lattice. Each conformation is weighted by its Boltzmann probability factor. We emphasize that this approach gives exact results within the mean field and lattice model approximations. No further approximations are needed to find the equilibrium distribution. Typical computation time is on the order of minutes on a desktop workstation. Parameters such as molecular weight, grafting density, and solvent quality can easily be varied, thus enabling the study of the grafted layer structure under various conditions. Therefore, a detailed comparison with analytical predictions is feasible.

The aim of this paper is a systematic comparison of the results obtained by the above-mentioned analytical and numerical SCF methods for a planar layer immersed in either a pure solvent or a solution of mobile polymer. An initial comparison of both approaches for the case of only an athermal solvent[17] was very promising. In this paper we consider a wide range of solvent strengths, including very good (better than athermal) and poor solvents.

The combination of these two different methods for the analysis of grafted layers is useful for several reasons. First, it provides a better understanding of the structural organization of grafted chain layers. Second, it enables us to check the validity of the assumptions made in the analytical theory, particularly the Newton approximation. Furthermore, the establishment of direct relationships between the analytical and the numerical results may stimulate further development of both models and their application to other systems.

In this paper we shall consider the equilibrium characteristics of a free, nondeformed planar layer, and its

0024-9297/92/2225-2657$03.00/0